ADVANCED MATERIALS TECHNOLOGIES
www.advmattechnol.de

A Single-Step Hot Embossing Process for Integration of Microlens Arrays in Biodegradable Substrates for Improved Light Extraction of Light-Emitting Devices

*Nils Jürgensen, Benjamin Fritz, Adrian Mertens, Jean-Nicolas Tisserant, Mathias Kolle, Guillaume Gomard, and Gerardo Hernandez-Sosa**

Integration of light management solutions relying on biodegradable materials in organic light-emitting devices could assist the development of sustainable light sources or conformable and wearable display technology. Using industrially relevant processing techniques, it is shown that microlens arrays can be seamlessly integrated into flexible and biodegradable cellulose diacetate substrates to facilitate extraction of the trapped substrate modes in light-emitting electrochemical cells. The substrates are patterned for light extraction and optimized for scalable printing processes in a single step by thermally embossing microlenses with polydimethylsiloxane molds on one substrate surface and simultaneous flattening of the other. Furthermore, by implementing the biopolymer substrate with microlens arrays, the total volume fraction of biodegradable materials in the microlense equipped device is 99.94%. The embossed microstructures on the biopolymer substrates are investigated by means of scanning electron microscopy and the angular light extraction profile of the devices is measured and compared to ray tracing simulations. Light-emitting electrochemical cells with integrated microlens array substrates achieve an efficiency enhancement factor of 1.45, exceeding conventional organic light-emitting diodes on glass substrates with laminated microlens arrays (enhancement factor of 1.23).

1. Introduction

Major technological advances in printed organic light-emitting devices in recent years have created new opportunities for cost-effective and high-throughput manufacturing methods using modern printing technologies.[1–6] Conveyed, modular production, individual and fast adjustment of designs, and compatibility with flexible and conformal substrates enable the development of new research fields and emerging markets for organic light-emitting devices. Particular promising is the increased utilization of biodegradable materials in organic light-emitting devices. Biodegradable light-emitting devices could improve advertisement or monitor the quality of products on sustainable disposable packaging.[7,8] Wearable bioelectronics could advance biomedical therapy and point-of-care diagnostics or even find use in transient electronics as well as in optogenetics.[9,10]

Various biodegradable electronic components, such as conductor paths,[11] energy-storing devices,[12,13] and logic elements,[14] have already been realized and single biodegradable constituents have been incorporated in photodiodes,[15] solar cells,[16] and light-emitting devices.[8] Deoxyribonucleic acid derivatives as transport and blocking layers,[17] insulin-amyloid-fibers for stearic stabilization,[18] or vitamin B2 derivatives as emitters[19] have been applied in the active layers of organic light-emitting diodes (OLED).[20] However, due to the fabrication complexity of multilayer OLED systems more

Dr. N. Jürgensen, B. Fritz, Dr. A. Mertens, Dr. G. Gomard, Dr. G. Hernandez-Sosa
Karlsruhe Institute of Technology-Light Technology Institute
Engesserstr. 13, 76131 Karlsruhe, Germany
E-mail: gerardo.sosa@kit.edu
Dr. N. Jürgensen, Dr. J.-N. Tisserant, Dr. G. Hernandez-Sosa
InnovationLab
Speyererstr. 4, 69115 Heidelberg, Germany
The ORCID identification number(s) for the author(s) of this article can be found under https://doi.org/10.1002/admt.201900933.

DOI: 10.1002/admt.201900933

Dr. J.-N. Tisserant
Braunschweig University of Technology-Institute for High Frequency Technology
Schleinitzstraße 22, 38106 Braunschweig, Germany
Prof. M. Kolle
Department of Mechanical Engineering
Massachusetts Institute of Technology
77 Massachusetts Avenue, Cambridge, MA 02139-4301, USA
Dr. G. Gomard
Karlsruhe Institute of Technology
Institute of Microstructure Technology
Eggenstein-Leopoldshafen, 76344 Karlsruhe, Germany

and more research is focused on light-emitting electrochemical cells (LEC).[21,22] LECs are capable of forming a p–i–n junction in situ by incorporation of salt ions in their single active layer. The reduced number of layers in an LEC is advantageous for printing applications[1,23] and also simplifies their implementation using biodegradable constituents. This is evident in recent reports on biodegradable solid polymer electrolytes formed from poly(lactic-*co*-glycolic acid) or polycaprolactone (PCL) and ionic liquids used in LECs.[24–26] In parallel, biodegradable substrates have recently received significant attention as enablers of more environmentally sustainable light technology. Substrates formed from silk,[27] chitin,[28] or cellulose[29–31] show excellent optical transparency, mechanical flexibility, and surface conditions for printing applications. Lately, these advancements resulted in fully printed LECs consisting to 99.98 vol% of biodegradable materials.[24] However, the use of biodegradable components tends to limit device performance, increasing the need for efficient management of the emitted light. Up to now, only a few reports have addressed light management in organic light-emitting devices using tailored biodegradable substrates.[32]

Generally in OLEDs, surface plasmon polaritons, waveguide-, and substrate-modes limit the light extraction efficiency of bottom emission devices to only around 20%.[33,34] To address this issue, the extraction of the substrate modes has been commonly addressed by various structural changes to the substrate–air interface.[35–38] One of the most prominent approaches is the use of substrates that are patterned with a microlens array (MLA). These arrays consist of lenses arranged in square,[39] hexagonal,[40,41] or disordered patterns,[42] which suppress total internal reflection that is usually prominent in planar substrates. MLAs are usually manufactured by hot embossing with polydimethylsiloxane (PDMS) stamps, which mold the structure into thermally deformable polymers or epoxides.[39–41,43–45] Hot embossing is commonly carried out either in polymer films deposited on glass substrates or on plastic foils, which are separately laminated onto the glass substrate.[43,44] MLA-enhanced OLED structures that enable the outcoupling of the substrate modes have achieved efficiency increases of 1.3 to 1.7 times compared to OLEDs without MLAs.[39–44] This efficiency lowers operation currents for organic light-emitting devices in order to obtain an equivalent luminance, which increases the operational lifetime and reduces power consumption. Furthermore, MLAs can help to increase the angular spread of the emitted light.

New approaches in the fabrication of MLAs have included the transfer of microstructures and microlenses on flexible substrates. In 2017, Yu et al. described a process where an adhesive was applied to a polyethylene terephthalate substrate, which was then embossed with a PDMS stamp.[45] However, this method can result in reflection losses at the substrate–MLA interface. To circumvent this issue, Xu et al. introduced OLEDs with flexible substrates and integrated photonic structures. The substrates were produced by spin coating a poly(amide acid) solution on microstructured glass templates followed by a baking process for thermal imidization to polyimide.[46] In this way, the substrate and the microstructures were made out of one piece and from the same material. However, the process had to be repeated several times to achieve stable substrate thicknesses and limited template sizes as well as long baking times were reported to slow down production.

Motivated by these efforts, we present in this work a hot embossing process to integrate MLAs in flexible transparent biodegradable substrates based on cellulose diacetate (CA). In combination with a previously reported flattening process on the device side of the substrate,[29] which reduces the root-mean-square roughness below 10 nm, we demonstrate enhanced substrate-mode extraction of up to 1.45 times relative to planar substrates. The MLAs were examined by optical and scanning electron microscopy, analyzed by ray tracing simulations and utilized as flexible substrates for LECs with inkjet-printed transparent electrodes. The angular emission was characterized and the efficiency enhancement was compared to conventional OLEDs on glass substrates with laminated MLA-foils.

2. Results and Discussion

2.1. Fabrication and Characterization of MLA-Foils

Due to the thermoplastic nature of CA with a glass transition temperature of 120 °C and to the excellent optical transparency in the visible range (see Figure S1, Supporting Information), CA-foils have already been successfully optimized for inkjet-printed electrodes in OLEDs and LECs by flattening the surface with a silicon wafer using pressure and heat.[24,29] Hence, hot embossing represented an ideal method to manipulate the topological structure of the material. MLAs were embossed on CA substrates (thickness: 500 µm, refractive index: 1.49) following the process described in **Figure 1**a. The biopolymer foils were placed between a silicon wafer and the PDMS mold. By increasing the temperature well above the

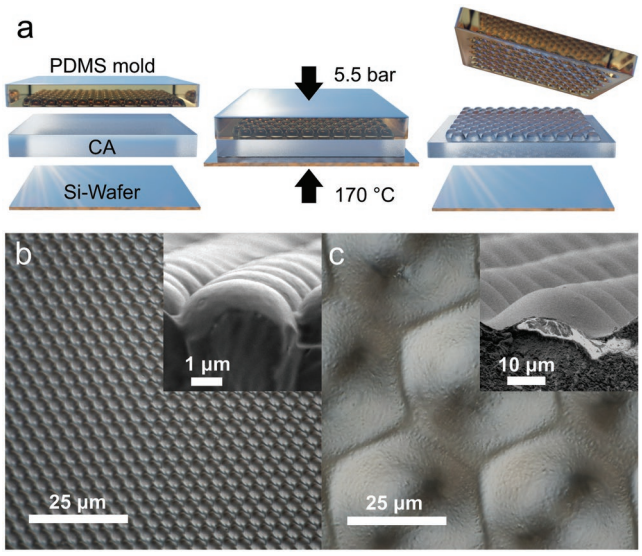

Figure 1. Hot embossing process of MLA on the CA substrates a). CA is sandwiched between a silicon wafer and the PDMS mold with the MLA-negative. Under applied pressure and elevated temperature, the microlenses are embossed into the biopolymer substrate and the reverse side is flattened. Top view optical micrographs of the SML b) and the LML c) on CA with the corresponding SEM-micrographs depicting the side view.

Table 1. Structural parameters for the MLAs in CA-substrates.

MLA	Diameter[a,b] [µm]	Height[b] [µm]	Aspect ratio[c]	Contact angle[b] [°]	Pitch size[a] [µm]	Fill factor [%]
SML	3.6	1.2	0.67	65	3.7	85.7
LML	37.1	10.4	0.56	41	38.6	83.7

[a]From microscopy micrographs; [b]From SEM; [c]Ratio of height to radius.

softening temperature of CA (127 °C) to 170 °C, the substrate foils became deformable. The MLAs were embossed into the polymer and the back side was simultaneously flattened against a planar silicon wafer. After cooling down to room temperature, the substrate with the integrated MLA can be detached and is ready to be used for further printing processes.

This process was used to produce hexagonal MLAs with either small microlens diameters (SMLs) of 3.6 µm or large microlens diameters (LMLs) of 37.1 µm. The embossed microlenses on CA were examined by optical and electron microscopy for a more detailed assessment of the structures' quality. Figure 1b,c shows the corresponding micrographs of the SML and LML, while insets show the corresponding cross section obtained by scanning electron microscopy (SEM). Here, the hemispherical shape of the SML and the parabolic shape of the LML are clearly visible. In **Table 1**, the individual parameters of the MLAs are listed (the parameters of the PDMS mold are included in the Supporting Information). The SMLs possess an aspect ratio (defined as the ratio of the height of the microlenses to their base radius) of 0.67 while the LMLs possess a smaller aspect ratio of 0.56. On the other hand, the contact angle (defined as the angle between the hemisphere and the flat surface) of the SML with 65° is larger than the angle of the LML with 41°. Simulations performed by Peng et al. have indicated that hemispherical microlenses with an aspect ratio of ≈1 show maximal light extraction.[41] Pan et al. have demonstrated that the maximum light extraction efficiency for hexagonally arranged parabolic microlenses is achieved with an aspect ratio of 0.72,[47] while Sun and Forrest have reported that larger contact angles increase light extraction.[40] The aspect ratio of the SML used here thus is not ideal but the larger contact angle should be favorable for better light extraction. Both MLAs (SML and LML) possess a fill factor of ≈83–85%, defined as the percentage of the total substrate area covered with microlenses, which is close to the ≈91% reported for ideal 2D hexagonal spherical packings.[44] Thus, the specifications of the replicated shapes of the microlenses on CA are well suited for light extraction in organic light-emitting devices.

2.2. Laminated MLA-Foils on OLEDs

In order to characterize the light extraction by the MLAs, reference devices were fabricated by optically coupling the structured CA-foils with an immersion oil (IMO) on the backside of conventional solution-processed OLEDs on indium tin oxide (ITO) covered glass substrates. The device setup is shown in **Figure 2**a. The OLEDs stack consisted of poly(3,4-ethylenedioxythiophene) polystyrene sulfonate (PEDOT:PSS) for hole injection, a commercial poly(p-phenylene-vinylene) derivate known as Super Yellow (SY) as emitter with a peak emission wavelength of 560 nm (see Figure S1, Supporting Information), and LiF and Al for electron injection and cathode, respectively. Figure 2b shows pixels during operation from the top, half of which are covered with either planar or structured CA-films. The unstructured CA-film shows an emission intensity that is hardly different from that of the uncoated glass substrate. In the case of SML, however, the edges of the pixel blur slightly and the light emission is more homogeneous. The difference between a flat surface and the microlenses is most obvious for the LML, in which light is more diffusely emitted and the width of the pixel is optically increased suggesting good light outcoupling.

The improved outcoupling of the light trapped in the glass substrates upon integration of MLAs was characterized by measuring the angle dependence of the electroluminescence (see Figure S2, Supporting Information). The normalized peak emission of SY as a function of emission angle is shown in **Figure 3**a. For reference, an ideal Lambertian emission is highlighted with gray crosses. The glass surface shows values slightly lower than the Lambertian emission at low emission angles while the flat CA-film values match the Lambertian emission for angles up to ≈30° which improve at larger angles. In comparison, the characteristics of the MLAs show a clear improvement in comparison to the flat references. To illustrate the corresponding spectral change, the change in light intensity

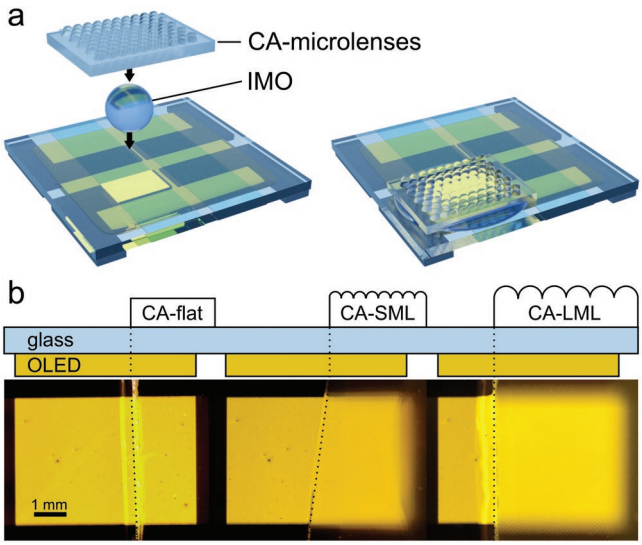

Figure 2. CA foils with microlenses are laminated with IMO to the backside of OLEDs (ITO/PEDOT:PSS/SY/LiF/Al) on glass substrates a). Top view macrographs of OLED pixels during operation with different CA foils partly covering the emitting area b).

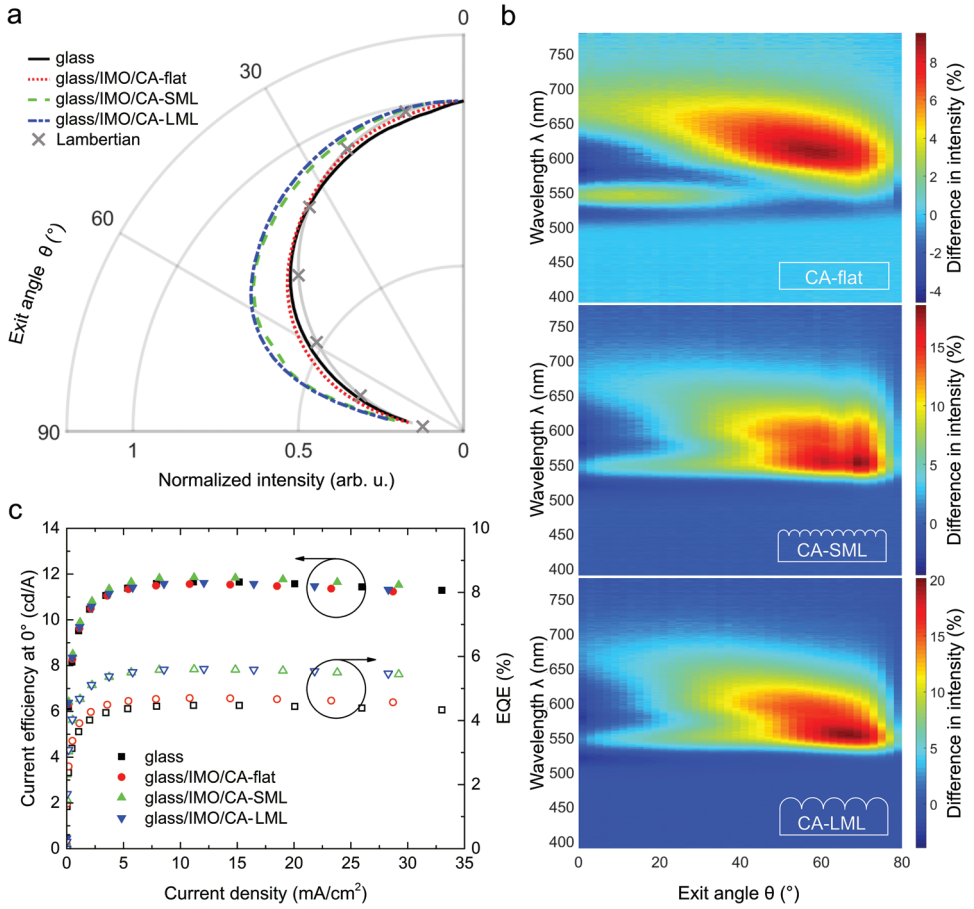

Figure 3. Exit angle-dependent maxima at 560 nm of the electroluminescence intensity, normalized at 0°, for different CA films laminated on the backside of OLEDs (ITO/PEDOT:PSS/SY/LiF/Al) with glass substrates. A Lambertian emission profile is given for reference with gray crosses a). Spectral difference of the electroluminescence intensities, normalized at the maximum at 0°, between different laminated CA foils and the bare glass substrate b). The measurements were done at 6.25 mA cm^{-2}. Current efficiency at a 0° exit angle (solid symbols) and the EQE of the different devices (open symbols), taking into account the light extraction over the entire half-space c).

of the different CA-films compared to the bare glass surface are shown in Figure 3b. The intensity difference refers to the maximum value of the measurement at 0°. In the case of the flat CA-film, only a slight increase of up to 8% in the range of 600–700 nm can be observed in the wavelength range of the maximum SY emission. In contrast, the intensity differences of the MLAs compared to glass show a uniform intensity increase over the entire spectral range with up to 20% for large exit angles. To quantify the increase in efficiency by the MLAs, we compared in Figure 3c the resulting device current efficiencies as a function of current density for an exit angle of 0°. These values were extracted from the luminance-current-voltage measurements shown in Figure S3, Supporting Information. The values for all samples are almost identical and approach a maximum of ≈12 cd A^{-1}, since the laminated MLAs only increase light extraction for larger exit angles, but not in normal direction. The overall improvement by utilizing MLAs is shown in the external quantum efficiency (EQE) presented in Figure 3c, which takes all light emitted in the forward half-space into account. Both the glass surface and the flat CA-film achieve values of 4.5–4.7%. The MLAs, on the other hand, increase the EQE of OLEDs to 5.6% by simple lamination on the glass substrate.

2.3. MLA-Foils as Substrates for LECs

Encouraged by the results of the laminated MLAs on glass substrates, we produced LECs on biodegradable CA-substrates with integrated MLAs as shown in **Figure 4**a (see photographs of the full devices in Figure S4, Supporting Information). Incorporating the biodegradable biopolymer as the substrate with a thickness of 500 µm enables mechanical flexibility, reduces the number of fabrication steps, and increases the overall volume fraction of biodegradable materials in the device to 99.94%. To fabricate the samples, highly conductive PEDOT:PSS was inkjet-printed as a transparent anode on the flattened side of the CA substrates. Subsequently, the emission layer consisting of SY as emitter, PCL as ion-dissolving polymer, and tetrahexylammonium tetrafluoroborate ($THABF_4$) as salt with a ratio of 1:0.05:0.2 for SY:PCL:$THABF_4$ was spin-coated, topped with an Ag cathode. The LECs were operated at a constant current density of 20.8 mA cm^{-2} and pixels in operation are shown in Figure 4b. For the flat surface, a homogeneous emission image was obtained, indicating that the PEDOT:PSS electrode is a pinhole-free and evenly printed layer.

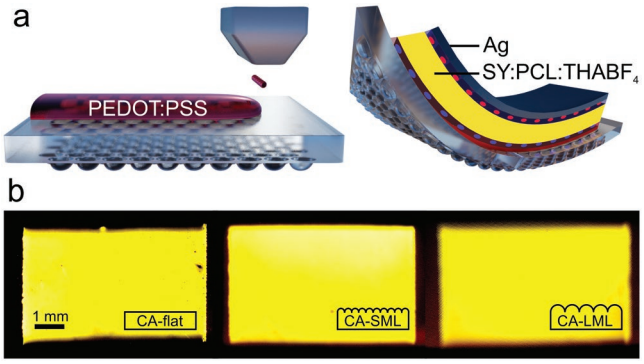

Figure 4. Structuring of a transparent anode of high conductive PEDOT:PSS by inkjet printing on CA-substrates with integrated MLA and the complete flexible LEC (PEDOT:PSS/SY:PCL:THABF$_4$/Ag) device stack with redistributed ions a). Macrographs of LEC pixels with different backside substrate surfaces during operation at a constant current density of 20.8 mA cm^{-2} b).

The normalized maxima of the SY-emission in **Figure 5**a present the light extraction differences of the LECs. It is immediately apparent that the intensity curve of the flat CA-substrate is clearly below that of a Lambertian emitter (see measurement in Figure S5, Supporting Information). In contrast, the LECs with MLAs show a much better light extraction compared to the flat substrate with the best results obtained for the SML. For comparison, the results of a ray tracing simulation of light extraction for a plane Lambertian SY-emitter radiating through the different CA-substrates is on the right side of Figure 5a. In agreement with the experimental results, a similar trend is observed, showing the strongest improvement for the SML, followed by the LML and a Lambertian emission for the flat surface. The experimentally determined intensity differences as a function of wavelength and exit angle between the MLAs and the flat CA-substrate are shown in Figure 5b. The intensity difference refers to the maximum value of the measurement at 0° of the flat CA sample. It is clearly observed that the MLAs amplify the light extraction over the entire width of the SY-emission spectrum. While the LML intensity increased by ≈17% in the range of 55° to 65°, the SML intensity rises by more than 25% between 60° and 70°. In order to quantify the efficiency improvement and account for the transient nature of LECs, the luminance behavior at an exit angle of 0° was measured for the first 10 min at a constant current density of 20.8 mA cm^{-2} (Figure 5c). It can be observed that LECs with MLAs achieve higher maximum luminance values of 470 cd m^{-2} than LECs with a flat substrate surface of only 430 cd m^{-2}. This shows that the light extraction of the CA-substrates is also improved in normal direction by means of MLAs. Accordingly, current efficiencies of ≈2.27 cd A^{-1} at 0° are achieved by the LECs with MLAs, while the LECs with flat surfaces achieve only 2.07 cd A^{-1}. The total improvement is finally reflected in the EQE shown in Figure 5c, since the EQE takes all photons emitted in the forward half-space into account. The LECs with a flat surface achieve the lowest values with a maximum EQE of ≈0.7%, while the SML and the LML samples achieve values around 1.0% and 0.9%, respectively.

A summary of all efficiencies and relative improvements to the OLED on glass and LEC on flat CA films is provided in **Table 2**. The overall increase in efficiency is considered in terms of the normal direction at 0° and as a function of emission angle. At 0°, laminated CA-films on glass with and without

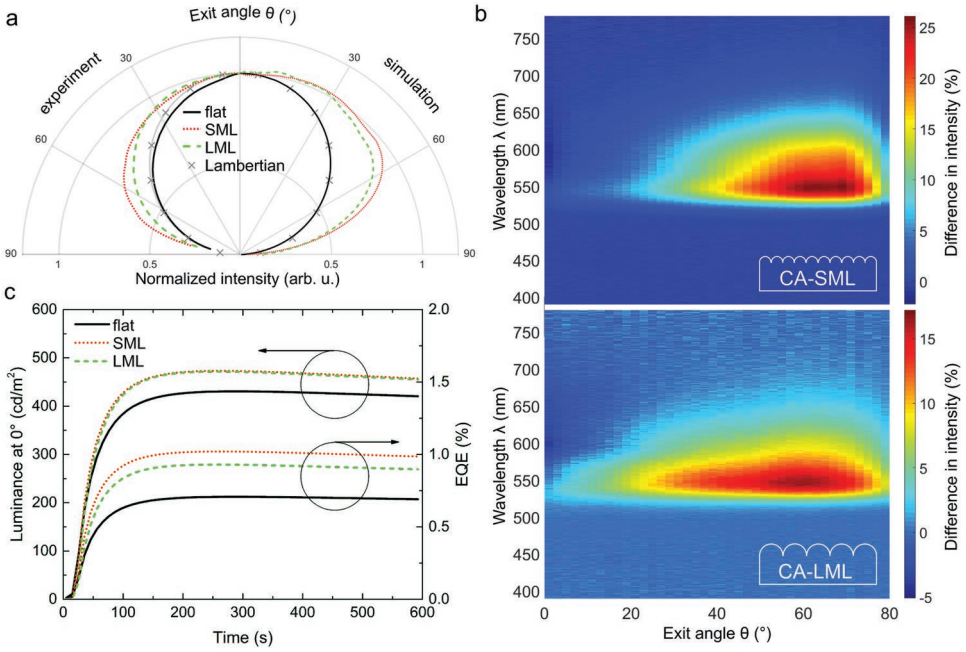

Figure 5. Exit angle-dependent maxima at 560 nm of the electroluminescence intensity, normalized at 0°, for LECs (PEDOT:PSS/SY:PCL:THABF$_4$/Ag) on CA substrates for different surfaces, measured (left) and simulated (right). A Lambertian emission profile is given for reference with gray crosses a). Spectral difference of the electroluminescence intensities, normalized to the maximum at 0°, between the CA-substrates with and without MLA b). Luminance turn-on characteristics for a constant current density of 20.8 mA cm^{-2} at 0° exit angle and the EQE for the different devices, taking into account the light extraction over the entire half-space c).

Table 2. Average efficiencies and increase in efficiency of OLEDs (ITO/PEDOT:PSS/SY/LiF/Al) and LECs (PEDOT:PSS/SY:PCL:$THABF_4$/Ag) for different substrates of at least four pixels on two different devices.

Device	Substrate	CE at 0° [cd A^{-1}]	EQE [%]	Increase in efficiency[a)]		
				at 0°	Angular	Half-space
OLED	Glass	11.7	4.5	Ref.	Ref.	Ref.
OLED	Glass/CA-flat	11.6	4.7	0.99	1.04	1.03
OLED	Glass/CA-SML	11.9	5.6	1.02	1.21	1.23
OLED	Glass/CA-LML	11.6	5.6	0.99	1.24	1.23
LEC	CA-flat	2.07	0.7	Ref.	Ref.	Ref.
LEC	CA-SML	2.27	1.0	1.10	1.32	1.45
LEC	CA-LML	2.26	0.9	1.09	1.22	1.33

[a)]Referring to the corresponding reference marked as Ref.

MLA cause no significant improvement of the OLED emission outcoupling compared to glass where only values of 0.99 to 1.02 are achieved. By integration of the angular measurement over the half space, the OLED/CA-flat sample only achieves a value of 1.04, but both the OLED/CA-SML and OLED/CA-LML show improvements in efficiency >20%. As a result, the overall efficiency increases by 1.03 times for flat surfaces and 1.23 times for CA-films with MLAs.

Correspondingly, the SML and LML CA-substrates for LECs show efficiency increases in the forward direction with factors 1.10 and 1.09, respectively, compared to the flat surface. Larger outcoupling improvements were observed in the angle-dependent measurements showing marked efficiency increases by factors of 1.32 and 1.22 corresponding to an overall efficiency increase by 1.45 times and 1.33 times for the SML and LML, respectively. These efficiency increases for the substrate-integrated MLAs outperform that of the laminated reference devices. Hence, CA-substrates with integrated MLAs demonstrate that this single-step process enables efficient light outcoupling by eliminating an extra interface between the substrate and the MLAs and the use of a higher refractive index substrate than glass.

3. Conclusion

We presented a hot embossing process, which equips flexible and biodegradable CA-substrates with hexagonal MLAs for substrate-mode extraction of LECs in a single step. This process creates substrates without an interface between the substrate and the MLA and favors light extraction compared to conventional laminating processes. The efficiency of LECs, structured by an inkjet process, was increased with a factor of up to 1.45 times through integration of MLAs into the substrate outperforming that of the laminated MLA reference. The presented approach simplifies the production of substrates with light management capabilities and can be transferred to typical hot-embossing processes used in industrial roll-to-roll production. Furthermore, the structure of the MLAs could be optimized for other optoelectronic applications, such as organic solar cells or photodiodes.

In summary, we have shown a universal approach for enhancing outcoupling in light-emitting devices by extending the functionality of a biodegradable substrate with MLAs with potential application in biocompatible or sustainable disposable display applications.

4. Experimental Section

Materials: All materials used were commercially purchased and used as received. Poly(3,4-ethylenedioxythiophene) polystyrene sulfonate (PEDOT:PSS, P VP AI 4083, F HC Solar) by Heraeus. Super Yellow (SY, Livilux PDY-132) and toluene (≥99.9%) by Merck. PCL (M_w = 14 000 g mol^{-1}), tetrahexylammonium tetrafluoroborate ($THABF_4$, ≥97%) by Sigma Aldrich. PDMS (Sylgard 184) by Dowsil. CA (500 µm, n = 1.49, oxygen transimission rate [OTR] = 73.8 cc m^{-2} day^{-1}) by Rachow Kunststoff-Folien GmbH. The SML-Master was manufactured by Maik Scherer at Papiermühlenfabrik Lousienthal. The LML-Master (MAF01) was acquired from Lumtec Lighting Corp. Pre-structured ITO-coated electronic grade glass (180 nm, 10 Ω $\square^{-1}$) by Kintec.

Fabrication and Characterization of CA-Substrates with MLA: PDMS Sylgard 184 resin by Dowsil was poured over the MLA-masters, cross-linked at 70 °C for 3 h and slowly removed to obtain the MLA-molds. The CA-foils were sandwiched between a clean Si-Wafer and the MLA-molds and hot embossed at 170 °C for 10 min at a pressure of 5.5 bar. They were subsequently released after cooling down to room temperature. The finished CA-substrates could then slowly be detached and used for further processing. The flat reference was produced by the same process, sandwiched between a clean Si-Wafer and a planar glass substrate. Hot embossing was done with a CNI Nanoimprinter from NIL Technology.

Optical micrographs were taken with a Nikon Eclipse 80i microscope and a focus stacking software Helicon Focus 7 by HeliconSoft. For the SEM-Images, the CA-foils were thermally evaporated with 100 nm of Ag at 10^{-6} mbar and broken in liquid nitrogen to observe a clear line of breakage. SEM pictures were acquired with an Auriga SEM by Zeiss.

Fabrication and Characterization of Light-Emitting Devices: For the OLEDs with glass substrates, prestructured ITO-glass was cleaned in acetone and 2-propanol within an ultrasonic bath for 10 min consecutively and then treated with oxygen plasma for 5 min. PEDOT:PSS (P VP AI 4083) was filtered with a 0.45 PVDF filter, spin coated at 3800 rpm for 30 s and annealed at 150 °C for 5 min to obtain films of 25 nm thickness. The samples were transferred into a nitrogen filled glovebox and spin-coated at 2000 rpm for 45 s with SY dissolved in toluene by 5 g L^{-1} to obtain films of 70 nm thickness. Afterward, 1 nm of LiF and 100 nm of Al were thermally evaporated through a shadow mask at 10^{-6} mbar yielding a 24 mm^2 active area. The backside of the glass substrate was then optically coupled to the CA-foils by an IMO (n = 1.5).

The LECs on the CA-substrates were produced as follows: the embossed CA-substrates were rinsed with 2-propanol and dried with

a nitrogen gun. PEDOT:PSS (F HC Solar) was filtered with a 0.45 filter and printed with a Dimatix DMP-2800 inkjet printer and a 10 pl Fujifilm Dimatix cartridge with a drop spacing of 30 µm to obtain films of 120 nm thickness. The films were dried at 10^{-2} mbar for 30 min and transferred to a nitrogen filled glovebox. SY, PCL, and $THABF_4$ were separately dissolved in toluene by 5 g L^{-1} mixed in the ratios 1:0.05:0.2 (SY:PCL:$THABF_4$). The solution was spin-coated at 2000 rpm for 45 s to obtain films of 70 nm thickness. Afterward, 100 nm of Ag was thermally evaporated through a shadow mask at 10^{-6} mbar yielding a 24 mm^2 active area.

For the angle-dependent measurements, the samples were encapsulated with glass and a transparent UV adhesive inside the nitrogen-filled glovebox. The angle dependent measurements were done in air with a XYZθ-Setup by Botest Systems and a Jaz spectrometer by Ocean Optics with a 2° step size at a current density of 6.25 mA cm^{-2} for the OLEDs and 20.8 mA cm^{-2} for the LECs with a 10 min pre-bias. The luminance-current-voltage characteristics were measured with a calibrated Botest LIV functionality test system inside the glovebox. The devices EQEs were calculated on the basis of the measured luminance-current characteristics and the angle-dependent spectra as explained elsewhere.[48,49]

Simulation: Combined ray tracing and transfer matrix method (TMM) calculations were carried out to simulate the outcoupling properties of the aforementioned LEC configuration. Commercial ray tracing software LightTools (Synopsys) was therefore used to simulate the angle (0°–89° in 1° steps) and polarization (s/p)-dependent reflectance of the LEC stack at a wavelength of 550 nm by TMM, where CA was chosen as the incident medium. In more details, the following layer stack (CA, incident medium, $n = 1.48$, $k = 0$; PEDOT:PSS, 160 nm, $n = 1.49$, $k = 0.0148$; SY:PCL:$THABF_4$, 70 nm, $n = 1.8$, $k = 0$; Ag, 100 nm, $n = 0.0533$, $k = 3.4848$) was implemented. The hereby obtained reflectance properties were then used to create a user-defined optical property ("coating") for LightTools 3D microtexture models depicting the small/large CA-MLA and a flat reference CA layer. The microlens models were implemented in the ray-tracing software by interpolating 3D surface data obtained with white light interferometry. The flat backside of the models was equipped with the user-defined reflectance behavior of the LEC thin film stack. A flat, homogeneous light source with a Lambertian emittance profile and a wavelength of 550 nm was placed inside the microtexture models to mimic the light-emitting behavior of the LEC at the bottom of the CA microlens foils. The light source emitted a total power of 1 W distributed over 10^8 rays into the CA material and a 4π far-field detector around the microtexture model was then used to calculate the total outcoupled power and the angular distribution of the outcoupled light rays.

Supporting Information

Supporting Information is available from the Wiley Online Library or from the author.

Acknowledgements

The authors acknowledge support from the German Federal Ministry of Education and Research (BMBF) through grand FKZ: 03X5526, the Karlsruhe School of Optics and Photonics (KSOP), the Karlsruhe House of Young Scientists (KHYS), the Helmholtz Postdoc Program, and the Humboldt foundation for funding. M.K. was supported in part by the US Army Research Office through the Institute for Soldier Nanotechnologies at MIT, under contract number W911NF-13-D-0001.

Conflict of Interest

The authors declare no conflict of interest.

Keywords

light-emitting electrochemical cells, light-management, microlens arrays, organic light-emitting diodes, sustainable electronics

Received: October 17, 2019
Revised: November 21, 2019
Published online:

[1] A. Sandström, A. Asadpoordarvish, J. Enevold, L. Edman, *Adv. Mater.* **2014**, *26*, 4975.
[2] A. Sandström, L. Edman, *Energy Technol.* **2015**, *3*, 329.
[3] G. Hernandez-Sosa, S. Tekoglu, S. Stolz, R. Eckstein, C. Teusch, J. Trapp, U. Lemmer, M. Hamburger, N. Mechau, *Adv. Mater.* **2014**, *26*, 3235.
[4] J. B. Preinfalk, T. Eiselt, T. Wehlus, V. Rohnacher, T. Hanemann, G. Gomard, U. Lemmer, *ACS Photonics* **2017**, *4*, 928.
[5] L. Zhou, L. Yang, M. Yu, Y. Jiang, C.-F. Liu, W.-Y. Lai, W. Huang, *ACS Appl. Mater. Interfaces* **2017**, *9*, 40533.
[6] L. Merklein, D. Daume, F. Braig, S. Schlisske, T. Rödlmeier, M. Mink, D. Kourkoulos, B. Ulber, M. Di Biase, K. Meerholz, G. Hernandez-Sosa, U. Lemmer, H. M. Sauer, E. Dörsam, P. Scharfer, W. Schabel, *Colloids Interfaces* **2019**, *3*, 32.
[7] M. Irimia-Vladu, *Chem. Soc. Rev.* **2014**, *43*, 588.
[8] E. Fresta, V. Fernández-Luna, P. B. Coto, R. D. Costa, *Adv. Funct. Mater.* **2018**, *28*, 1707011.
[9] S. I. Park, D. S. Brenner, G. Shin, C. D. Morgan, B. A. Copits, H. U. Chung, M. Y. Pullen, K. N. Noh, S. Davidson, S. J. Oh, J. Yoon, K.-I. Jang, V. K. Smineni, M. Norman, J. G. Grajales-Reyes, S. K. Vogt, S. S. Sundaram, K. M. Wilson, J. S. Ha, R. Xu, T. Pan, T. Kim, Y. Huang, M. C. Montana, J. P. Golden, M. R. Bruchas, R. W. Gereau IV, J. A. Rogers, *Nat. Biotechnol.* **2015**, *33*, 1280.
[10] M. Mehrali, S. Bagherifard, M. Akbari, A. Thakur, B. Mirani, M. Mehrali, M. Hasany, G. Orive, P. Das, J. Emneus, T. L. Andresen, A. Dolatshahi-Pirouz, *Adv. Sci.* **2018**, *5*, 1700931.
[11] S.-W. Hwang, H. Tao, D.-H. Kim, H. Cheng, J.-K. Song, E. Rill, M. A. Brenckle, B. Panilaitis, S. M. Won, Y.-S. Kim, Y. M. Song, K. J. Yu, A. Ameen, R. Li, Y. Su, M. Yang, D. L. Kaplan, M. R. Zakin, M. J. Slepian, Y. Huang, F. G. Omenetto, J. A. Rogers, *Science* **2012**, *337*, 1640.
[12] L. Yin, X. Huang, H. Xu, Y. Zhang, J. Lam, J. Cheng, J. A. Rogers, *Adv. Mater.* **2014**, *26*, 3879.
[13] X. Wang, W. Xu, P. Chatterjee, C. Lv, J. Popovich, Z. Song, L. Dai, M. Y. S. Kalani, S. E. Haydel, H. Jiang, *Adv. Mater. Technol.* **2016**, *1*, 1600059.
[14] M. Irimia-Vladu, E. D. Glowacki, G. Schwabegger, L. Leonat, H. Z. Akpinar, H. Sitter, S. Bauer, N. S. Sariciftci, *Green Chem.* **2013**, *15*, 1473.
[15] J.-W. Choi, Y.-S. Nam, W.-H. Lee, D. Kim, M. Fujihira, *Appl. Phys. Lett.* **2001**, *79*, 1570.
[16] R. Nie, A. Li, X. Deng, *J. Mater. Chem. A* **2014**, *2*, 6734.
[17] J. A. Hagen, W. Li, A. Steckl, J. Grote, *Appl. Phys. Lett.* **2006**, *88*, 171109.
[18] H. Tanaka, A. Herland, L. J. Lindgren, T. Tsutsui, M. R. Andersson, *Nano Lett.* **2008**, *8*, 2858.
[19] N. Jürgensen, M. Ackermann, T. Marszalek, J. Zimmermann, A. J. Morfa, W. Pisula, U. H. Bunz, F. Hinkel, G. Hernandez-Sosa, *ACS Sustainable Chem. Eng.* **2017**, *5*, 5368.
[20] C. Tang, S. VanSlyke, *Appl. Phys. Lett.* **1987**, *51*, 913.
[21] Q. Pei, G. Yu, C. Zhang, Y. Yang, A. J. Heeger, *Science* **1995**, *269*, 1086.
[22] S. Tang, L. Edman, in *Photoluminescent Materials and Electroluminescent Devices*, Springer, Cham, Switzerland **2017**, pp. 375–395.

[23] G. Hernandez-Sosa, A. Morfa, N. Jürgensen, S. Tekoglu, J. Zimmermann, in *Light-Emitting Electrochemical Cells* (Ed: R. Costa), Springer, Cham, Switzerland **2017**, pp. 139–163.
[24] J. Zimmermann, L. Porcarelli, T. Rödlmeier, A. Sanchez-Sanchez, D. Mecerreyes, G. Hernandez-Sosa, *Adv. Funct. Mater.* **2018**, *28*, 1705795.
[25] J. Zimmermann, N. Jürgensen, A. J. Morfa, B. Wang, S. Tekoglu, G. Hernandez-Sosa, *ACS Sustainable Chem. Eng.* **2016**, *4*, 7050.
[26] N. Jürgensen, J. Zimmermann, A. J. Morfa, G. Hernandez-Sosa, *Sci. Rep.* **2016**, *6*, 36643.
[27] Y. Liu, Y. Xie, Y. Liu, T. Song, K.-Q. Zhang, L. Liao, B. Sun, *Semicond. Sci. Technol.* **2015**, *30*, 104004.
[28] J. Jin, D. Lee, H.-G. Im, Y. C. Han, E. G. Jeong, M. Rolandi, K. C. Choi, B.-S. Bae, *Adv. Mater.* **2016**, *28*, 5169.
[29] A. Morfa, T. Rödlmeier, N. Jürgensen, S. Stolz, G. Hernandez-Sosa, *Cellulose* **2016**, *23*, 3809.
[30] S.-H. Min, C. K. Kim, H.-N. Lee, D.-G. Moon, *Mol. Cryst. Liq. Cryst.* **2012**, *563*, 159.
[31] D. Ha, Z. Fang, N. B. Zhitenev, *Adv. Electron. Mater.* **2018**, *4*, 1700593.
[32] H. Zhu, Z. Fang, Z. Wang, J. Dai, Y. Yao, F. Shen, C. Preston, W. Wu, P. Peng, N. Jang, Q. Yu, Z. Yu, L. Hu, *ACS Nano* **2016**, *10*, 1369.
[33] M. C. Gather, S. Reineke, *J. Photonics Energy* **2015**, *5*, 057607.
[34] G. Gomard, J. B. Preinfalk, A. Egel, U. Lemmer, *J. Photonics Energy* **2016**, *6*, 030901.
[35] T. Fujii, Y. Gao, R. Sharma, E. Hu, S. DenBaars, S. Nakamura, *Appl. Phys. Lett.* **2004**, *84*, 855.
[36] T. Tsutsui, M. Yahiro, H. Yokogawa, K. Kawano, M. Yokoyama, *Adv. Mater.* **2001**, *13*, 1149.
[37] G. Gu, D. Z. Garbuzov, P. E. Burrows, S. Venkatesh, S. R. Forrest, M. E. Thompson, *Opt. Lett.* **1997**, *22*, 396.
[38] T. Yamasaki, K. Sumioka, T. Tsutsui, *Appl. Phys. Lett.* **2000**, *76*, 1243.
[39] S. Möller, S. Forrest, *J. Appl. Phys.* **2002**, *91*, 3324.
[40] Y. Sun, S. R. Forrest, *J. Appl. Phys.* **2006**, *100*, 073106.
[41] H. Peng, Y. L. Ho, X.-J. Yu, M. Wong, H.-S. Kwok, *J. Disp. Technol.* **2005**, *1*, 278.
[42] F. Galeotti, W. Mróz, G. Scavia, C. Botta, *Org. Electron.* **2013**, *14*, 212.
[43] S.-H. Eom, E. Wrzesniewski, J. Xue, *Org. Electron.* **2011**, *12*, 472.
[44] M.-K. Wei, J.-H. Lee, H.-Y. Lin, Y.-H. Ho, K.-Y. Chen, C.-C. Lin, C.-F. Wu, H.-Y. Lin, J.-H. Tsai, T.-C. Wu, *J. Opt. A: Pure Appl. Opt.* **2008**, *10*, 055302.
[45] R. Yu, F. Yin, X. Huang, W. Ji, *J. Mater. Chem. C* **2017**, *5*, 6682.
[46] Z. Xu, M. Li, M. Xu, J. Zou, H. Tao, L. Wang, J. Peng, *Org. Electron.* **2017**, *44*, 225.
[47] C. Pan, Y. Chen, M. Chen, Y. Hsu, *Opt. Commun.* **2011**, *284*, 3323.
[48] S. Okamoto, K. Tanaka, Y. Izumi, H. Adachi, T. Yamaji, T. Suzuki, *Jpn. J. Appl. Phys.* **2001**, *40*, L783.
[49] T. Tsutsui, K. Yamamato, *Jpn. J. Appl. Phys.* **1999**, *38*, 2799.